Mathematical Biosciences and Engineering

MBE, 18 (6): 7648–7665.
DOI: 10.3934/mbe.2021379
Received: 29 May 2021
Accepted: 26 August 2021
Published: 06 September 2021

http://www.aimspress.com/journal/MBE

Research article

Investigating two kinds of cellular alternans and corresponding TWA induced by impaired calcium cycling in myocardial ischemia

Jiaqi Liu†, Zhenyin Fu†, Yinglan Gong and Ling Xia*

Key Laboratory for Biomedical Engineering of Ministry of Education, Institute of Biomedical Engineering, Zhejiang University, Hangzhou 310027, China

* **Correspondence:** Email: xialing@zju.edu.cn.

† These authors contributed equally to this paper.

Abstract: *Background***:** The utility of T wave alternans (TWA) in identifying arrhythmia risk has been demonstrated. During myocardial ischemia (MI), TWA could be induced by cellular alternans. However, the relationship between cellular alternans patterns and TWA patterns in MI has not been investigated thoroughly. *Methods:* We set MI conditions to simulate alternans. Either prolonging Ca^{2+} release or increasing spark-induced sparks (secondary sparks) can give rise to different patterns of APD alternans and TWA. In addition, different ischemic zones and reduced conduction velocity are also considered in one dimensional simulation. *Results:* Delay of Ca^{2+} release can produce discordant Ca^{2+}-driven alternans in single cell simulation. Increasing secondary sparks leads to concordant alternans. Correspondingly, morphology and magnitude of TWA vary in two different cellular alternans. Epi ischemia results in alternans concentrating in the first half of T wave. Endo and transmural ischemia lead to fluctuations in the second half of T wave. In addition, slowing conduction velocity has no effect on TWA magnitude. *Conclusion:* Specific ionic channel dysfunction and ischemic zones affect TWA patterns.

Keywords: alternans; Ca^{2+} release; TWA; ischemia

1. Introduction

Myocardial ischemia (MI) causes electrical alternans [1–5], which refer to beat-to-beat alternans in action potential duration (APD) or/and Ca^{2+} transient in the cellular level [6–9] and T wave alternans

(TWA) on the electrocardiogram (ECG) in the tissue level [10]. Cardiac alternans have been shown to lead fatal arrhythmia, where TWA is confirmed to have promising utility in risk prediction of sudden cardiac death (SCD) and could be considered as a strong marker of arrhythmia [11–13]. To make full use of TWA, making clear of the underlying mechanism forming it is essential in clinical. As T wave reflects transmural repolarization dispersion, TWA are thought to arise from repolarization differences in tissue heterogeneity [14,15], conduction velocity [16,17] and cellular alternans [3,13,18–20]. Cellular alternans and TWA are investigated by a plethora of studies from various perspectives [9,21–24].

With respect to cellular alternans, controversy arises from the unsolved chicken-or-egg problem: which of APD alternans and Ca^{2+} alternans occur first [24]? Ca^{2+} alternans can be induced by applying alternans AP-clamp protocol, which is membrane voltage (V_m)-driven alternans [25,26]. Fluctuation of sarcoplasmic reticulum (SR) Ca^{2+} ($[Ca^{2+}]_{sr}$) could trigger Ca^{2+} alternans, which is Ca^{2+}-driven alternans [9,21]. The fact that alternans arising from either genesis could happen, along with the bidirectional coupling between Ca^{2+} transient and V_m [9,15,21,27] complicates the chicken-or-egg problem.

As to differentiate the two mechanisms, a method of constant-diastolic-interval-pacing is put forward [28]. When applying constant diastolic interval (DI), Ca^{2+}-driven alternans could not be eliminated until the strength of calcium instability is reduced. Therefore, finding out the factors associate with calcium stability becomes vital in investigating Ca^{2+} alternans. Furthermore, researchers expand this constant-DI-pacing method to constant-TR-pacing method, which implements constant TR interval in one cable simulation [29]. Both of the two methods contribute to prevent alternans with cycle length (CL) larger than 250 ms. Significantly, calcium handlings could be affected whenever CL is more or less than 250 ms due to voltage-calcium coupling and deserves more investigation.

Cellular alternans could be divided into concordant and discordant [9,21,27]. When a large Ca^{2+} transient gives rise to a long APD, this alternans is called concordant. Correspondingly, discordant alternans indicates a small Ca^{2+} transients paralleled by a long APD. Due to the bidirectional coupling between Ca^{2+} dynamics and V_m, Ca^{2+}-related currents, such as L-type calcium current (I_{CaL}) and Na^+-Ca^{2+} exchange current (I_{NaCa}) make a difference in forming the two different alternans [9,21,27]. Although the effects of the two currents on APD alternans have been investigated, how the two different alternans affect TWA forming remains unknown.

As to TWA, we mainly care about its utility and value in clinical. A lot of studies aim to build relationship between TWA and prediction of SCD [30,31]. Particularly, TWA is a strong marker of arrhythmia in patients with ischemic heart disease. Prognostic value of TWA test is also confirmed after MI [4]. The magnitude of TWA is associated with heterogeneity of repolarization, which is the key factor to predict arrhythmia [11,12]. Ischemia is considered to increase the magnitude of TWA [11]. Meanwhile, ischemia is shown to produce beat-to-beat variations in peak-systolic and end-diastolic cytosolic Ca^{2+} ($[Ca^{2+}]_i$) [6,7], alternans in amplitudes and durations of V_m [17]. Moreover, there could be 2:1 response of monophasic potential according to unipolar extracellular electrogram [17]. Various methods analyzing TWA are put forward to broaden the usage of TWA in clinical. However, there is no detailed analysis of ischemia-induced alternans forming from ionic basis to cellular level and eventually to the tissue level.

The ionic basis for cellular alternans could play an important role in explaining how TWA occur, providing valuable information in investigating risk prediction of SCD. However, the underlying mechanisms forming TWA vary from abnormal ionic currents and other electrical factors [12]. In heart failure, a steep fractional Ca^{2+} release determines the occurrence of alternans [32]. The balance between calcium uptake and release could be disrupted when heart rate is elevated [11]. TWA induced

by myocardial ischemia is considered with calcium cycling. In all, calcium cycling and Ca^{2+}-related currents involved in voltage-calcium coupling exert essential influence on alternans occurrence. Finding out key factors forming cellular alternans is essential, which contributes to explain the characteristics of TWA broaden its use in therapy.

To investigate ischemia-induced TWA mechanism, we simulate cellular alternans and TWA in one dimensional cable in ischemia. MI includes hyperkalemia, acidosis, and anoxia [33,34]. Hyperkalemia is shown to be related with depolarization phase [35] and QRS wave on ECG. Acidosis decreases the amplitudes of depolarizing current I_{Na}, and I_{CaL} [34]. Anoxia reduces cytosolic ATP, resulting in opening ATP sensitive potassium current (I_{KATP}) [36]. Acidosis along with anoxia impair sarcoplasmic reticulum Ca^{2+} pump (SERCA) functioning [37] and change properties of ryanodine receptors (RyRs) [38]. I_{NaCa} is reduced or even becomes to be in reverse mode [34]. In addition, diastolic $[Ca^{2+}]_i$ and net magnitudes of Ca^{2+} transients are increased during ischemia [6,39].

On the one hand, we aim to simulate both concordant and discordant Ca^{2+}-driven alternans in ischemia and analyze factors in affecting alternans forming. On the other hand, different ischemic zones and reduced conduction velocity are set to find out factors affect TWA patterns. Clinical data show TWA could be centered on the first half of T waves [40,41], however, no explanations are given in forming this alternans. We aim to build the link between cellular alternans and TWA patterns, broadening TWA utility in clinical.

2. Methods

2.1. Impaired Ca^{2+} uptake pump

The Ca^{2+} uptake rate is decreased during ischemia [37]. A thermodynamic Ca^{2+} uptake pump model was used to be integrated into human ventricular cell model [42] (Ord model). Then the integrated model was applied to one dimensional cable to get ischemic p-ECG with CL of 700 ms. The uptake rate was multiplied by an appropriate coefficient of C_{up}, making the amount of retaken Ca^{2+} minus leaked Ca^{2+} in integrated model almost as the same with that in original Ord model.

2.2. Two types of Ca^{2+} transients

Ischemia is confirmed to induce Ca^{2+} alternans by modulating Ca^{2+} dynamics. Here Ca^{2+} alternans patterns were mainly decided by changes in properties of RyR channels. There are three properties of Ca^{2+} release channel, randomness, refractoriness and recruitment [43]. Either prolonging the refractory period or increasing the frequency of spark-induced sparks (which is also called secondary sparks [43]) contributes to alternans. According to changes in the two properties, we modified the formula of Ca^{2+} release current, respectively. In type I, time constants of all the RyRs (τ_{rel}) channels were increased by 80 ms to simulate prolonged refractory period. In type II, a new gate of O_r was added to the formula, controlling the occurrence of secondary sparks. The value of O_r depends on $[Ca^{2+}]_{jsr}$ and ranges from zero to one, representing the probability of secondary sparks occurring. The time constant of this gate O_r is regulated by I_{CaL}.

$$O_{rss} = 0.1 + \frac{0.9}{1+\frac{e^{-Ca_{jsr}+Ca_{jsr1}}}{0.001}} + \frac{0.1}{1+\frac{e^{-Ca_{jsr}+Ca_{jsr2}}}{0.5}} \quad (1)$$

$$\tau_{Or} = \frac{1}{0.01+\frac{0.01}{0.001+I_{CaL}}} \quad (2)$$

2.3. Ischemic settings

2.3.1. Transmural ischemia

We also modified formula of Ca^{2+} release current in Endo and M cell model, respectively. These modifications were aimed to decrease ischemic level from Endo cells to Epi cells, simulating coronary artery occlusion. Detailed transmural ischemic parameters were shown in Table 1.

Table 1. Ischemic transmural cells.

	Endo	M	Epi
I_{Na}	85%	90%	95%
I_{CaL}	85%	90%	95%
I_{NaCa}	50%	60%	70%
C_{up}	0.00508	0.007275	0.008992
$[ATP]_i$ (mM)	3.8	5.3	6.8
$[ADP]_i$ (mM)	0.025	0.02	0.015
$[Pi]_i$ (mM)	15	10	5
$[PH]_i$	7	7	7.1
$[Ca^{2+}]_{jsr1}$ (mM)	1.421	2.031	2.221
$[Ca^{2+}]_{jsr2}$ (mM)	1.422	2.032	2.222

2.3.2. Epi ischemia

During Epi ischemia, we simulated TWA induced by two patterns of Ca^{2+} alternans, respectively. Except for the difference in formula of Ca^{2+} release current, we set other ischemic parameters as the same. I_{Na}, I_{CaL} and I_{NaCa} were reduced to 95%, 95% and 70%, respectively; $[ATP]_i$, $[ADP]_i$, $[Pi]_i$ and $[PH]_i$ were set 6.8 mM, 15 mM, 5 mM, and 7.1. I_{KATP} and Ca^{2+} uptake current (J_{up}) were affected by the same ischemic conditions.

2.3.3. Endo ischemia

To investigate the effect of ischemic zone on TWA, we simulated p-ECG during Endo ischemia, where ischemic parameters are shown in Table I and cellular alternans are induced by adding the gate O_r.

2.4. p-ECG

One dimensional cable was used to simulate p-ECG in control, Epi ischemia, Endo ischemia and transmural ischemia. 60 Endo cells, 45 M cells and 60 Epi cells are connected to form this fiber. As the part of atrium was missing in our cable, P-wave representing the activation of atrium was lacking in p-ECG. The length of each cell was set as 0.01cm and p-ECG was calculated at the point 3.65 cm far from the first Endo cell [35]. Electrical coupling between neighboring cells was expressed as the

following equation, where the value of D was 0.154 $mm^2\ ms^{-1}$, representing the tensor of diffusion coefficient along the fiber [35]. In addition, I_{stim}, I_{ion} and C_m are current stimulus, ionic currents and membrane capacity respectively.

$$\frac{\partial V_m}{\partial t} = -\frac{I_{stim}+I_{ion}}{C_m} + D \cdot \nabla^2 V_m \tag{3}$$

3. Results

3.1. Two types of Ca^{2+} alternans

We simulated concordant alternans (Type I) and discordant alternans (Type II). Type I is as shown in Figure 1, diastolic Ca^{2+} concentration alternates slightly (Figure 1a) and Ca^{2+} release current (J_{rel}) alternates in magnitude (Figure 1c). In type II, alternans in diastolic Ca^{2+} concentration is evident (Figure 1b) and a large Ca^{2+} release occurs in every two beats (Figure 1d).

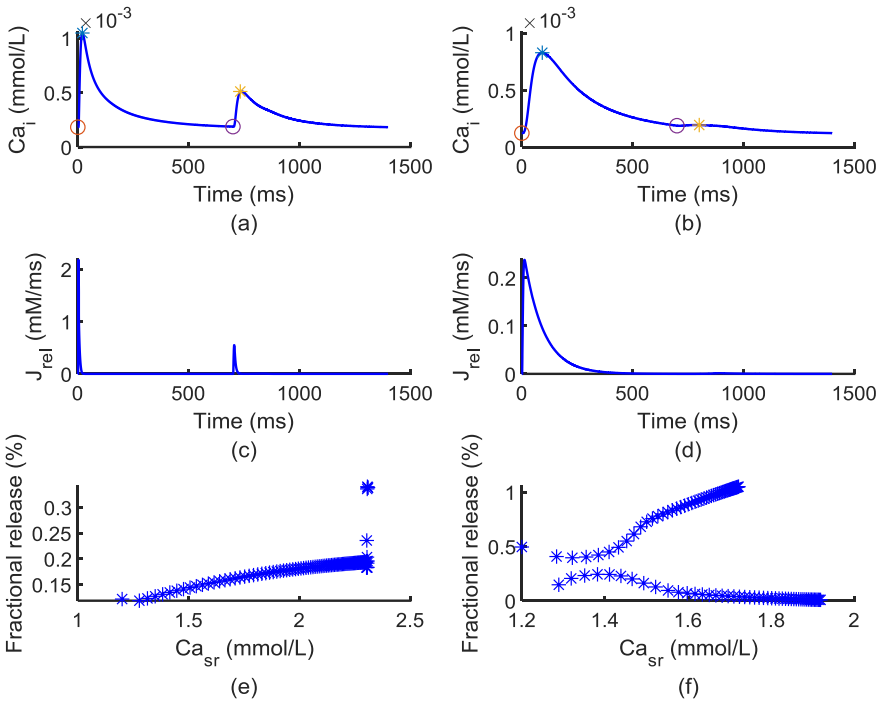

Figure 1. $[Ca^{2+}]_i$, J_{rel} alternans and fractional Ca^{2+} release curve in type I and II Ca^{2+} alternans. Where asterisk (*) represents the amplitude of Ca^{2+} transient in one beat and hollow circle (o) marks the diastolic $[Ca^{2+}]_i$ (1a and 1b).

To evaluate the degree of Ca^{2+} alternans, Ca^{2+} alternans ratio is introduced. Ca^{2+} alternans ratio is defined as the value of 1-B/A, where B and A are net magnitudes of small and large Ca^{2+} transients respectively [7]. The mean values of alternans ratios in two types were calculated for ten beats in stable state and given in Table 2. The value of alternans ratio in type II is larger than in type I, indicating that fluctuations of Ca^{2+} transients are more evident in type II.

Table 2. The difference of time duration completing 60% and 90% repolarization in two types of Ca2+ alternans.

	DAPD60	DAPD90	Ca^{2+} alternans ratio
Type I	2.9726	3.4726	0.6269
Type II	-21.4192	-10.6172	0.9919

Steep fractional Ca^{2+} release curve plays a key role in forming Ca^{2+} alternans. Here we recorded the relationship between the fractional released Ca^{2+} and sarcoplasmic reticulum Ca^{2+} concentration ($[Ca^{2+}]_{sr}$) during 100 beats, where the initial of $[Ca^{2+}]_{sr}$ is 1.2 mmol/l (Figure 1e). According to Figure 1e, Ca^{2+} release is small with $[Ca^{2+}]_{sr}$ lower than the threshold of 1.7 mmol/l. When $[Ca^{2+}]_{sr}$ comes to the threshold, a small increase will result in large Ca^{2+} release, which indicates O_r gate becomes massively open. Figure 1f shows that bifurcations exist from the beginning of recording.

3.2. Corresponding APD alternans, TWA

Two types of APD alternans are shown in Figure 2a,b. In Figure 2a, although we could not tell evident alternans in APD of type I, partially enlarged view shows there are slight difference between APDs. In type II, a very small Ca^{2+} transient causes I_{CaL} to last longer (Figure 2d). Correspondingly, plateau phases alternate evidently (Figure 2b).

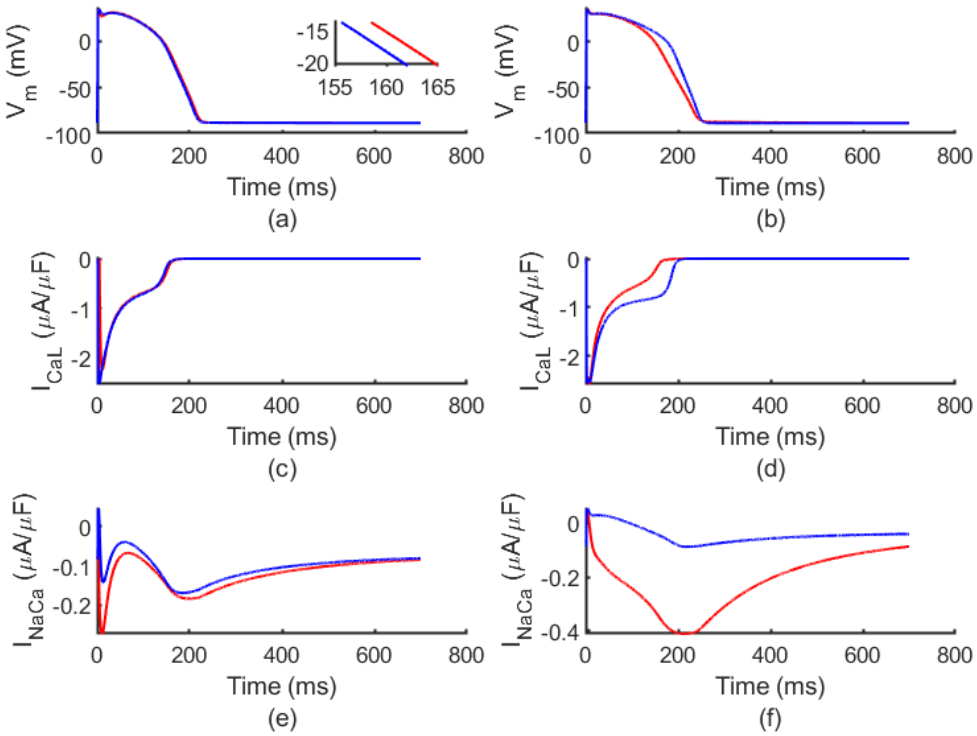

Figure 2. APDs, I_{CaL} and I_{NaCa} in type I and II Ca^{2+} alternans. Where the first beat is shown in red line and the second is in blue line.

During Ca^{2+}-driven alternans, I_{CaL} and I_{NaCa} are key factors transforming Ca^{2+} alternans to APD alternans. Both currents also affect repolarization durations in different phases. Here, durations of repolarization and repolarizing currents (I_{CaL} and I_{NaCa}) are picked up and compared. We recorded the time duration completing 60% and 90% of repolarization (APD_{60} and APD_{90}) in every beat and calculated the difference of them ($DAPD_{60}$ and $DAPD_{90}$) between every two consecutive beats. $DAPD_{60}$ ($DAPD_{90}$) is calculated by subtracting APD_{60} (APD_{90}) of the second beats from that of the first beats.

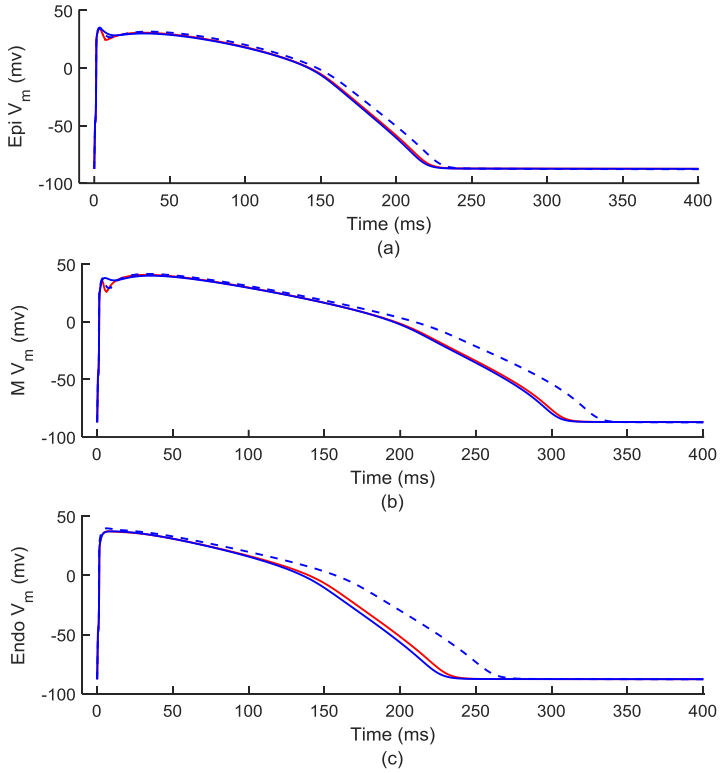

Figure 3. APD alternans of Epi cell (a), M cell (b) and Endo cell (c), where cellular alternans are produced by adding the Or gate. The first beat is shown in red line and the second is in blue line. The blue dashed lines represent APDs in control.

Table 2 gives mean values of them in two types. Positive values indicate APDs are longer in the first beats than in the second beats. Table 2 shows that $DAPD_{90}$ is larger than $DAPD_{60}$ in type I alternans and the absolute value of $DAPD_{90}$ is smaller than $DAPD_{60}$ in type II. Where, $DAPD_{60}$ and $DAPD_{90}$ are mainly influenced by alternans through I_{CaL} and I_{NaCa}. A small Ca^{2+} transient results in large I_{CaL} (Figure 2c,d) and small I_{NaCa} (Figure 2e,f), having contrasting effects on the repolarization duration. Note that in the second beat of type II alternans, although the small I_{NaCa} contributes to shorten repolarization duration, the prolongation of plateau phase plays a dominant role in the long APD. That indicates I_{CaL} lasting longer than in the first beat. Whereas in type I, the small I_{NaCa} plays a dominant role in all the repolarization phases in the first beat, resulting in a shorter APD. Moreover, the durations I_{CaL} lasting for are almost the same during the two consecutive beats. The difference in durations of I_{CaL} plays a dominant role in deciding alternans patterns.

In all, when there is a large Ca^{2+} transient in type II Ca^{2+} alternans (Figure 1b), the corresponding APD is short (Figure 2b), which is shown as discordant alternans. Whereas type I is concordant alternans.

T wave arises from the difference of repolarization durations between transmural cells. Repolarization starts from Epi cells to M and Endo cells. When T wave reaches to its peak (Figure 4a), the difference between transmural cells repolarization durations increases to the maximum. Figure 5a shows Epi ischemia induces larger T wave magnitudes, indicating the heterogeneity of transmural repolarization is increased. To investigate how the repolarization heterogeneity is affected by these two types of alternans, we compare the APDs in control conditions and that in ischemia (Figure 3). Repolarization durations are shortened by I_{KATP} during ischemia. Correspondingly, the time when the magnitude of T wave reaches is earlier in all ischemic conditions than under control.

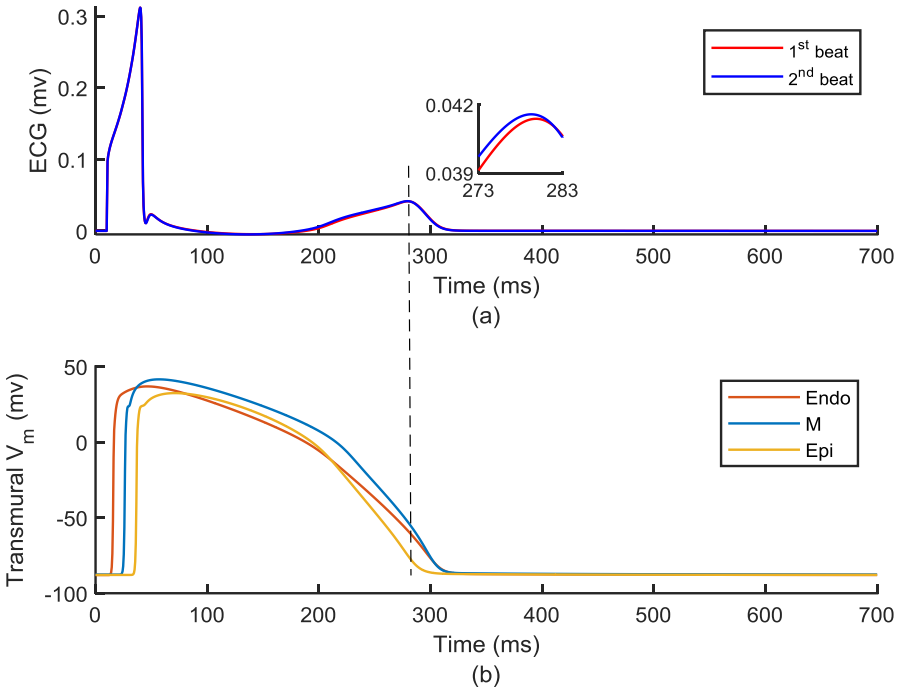

Figure 4. P-ECG and APDs under control. (a). P-ECG. (b). APDs of Endo cell (the 35th cell of the fiber), M cell (85th) and Epi cell (135th).

To compare the effect of ischemic zone on TWA patterns, we simulated p-ECG during Epi ischemia, and Endo ischemia, where cellular alternans was concordant alternans. In control conditions, T waves show very slight alternans (Figure 4a). We set initial values of transmural cell models, making them come to stable state in single cell simulation. The cable simulation with our initial values takes time to become stable and thus there is small fluctuations of T waves (Figure 4a). Figures 5–8 show that TWA patterns change with different ischemic zones and cellular alternans patterns.

Type I alternans of Epi induced by ischemia could not result in obvious TWA (Figure 5a). Note that the time when J point appears is different during the two consecutive beats. In the first beat, J point appears early, which means repolarization of the cable starts early. Correspondingly, Figure 5c shows in the first beat, Epi completes depolarization phase earlier than in the second beat.

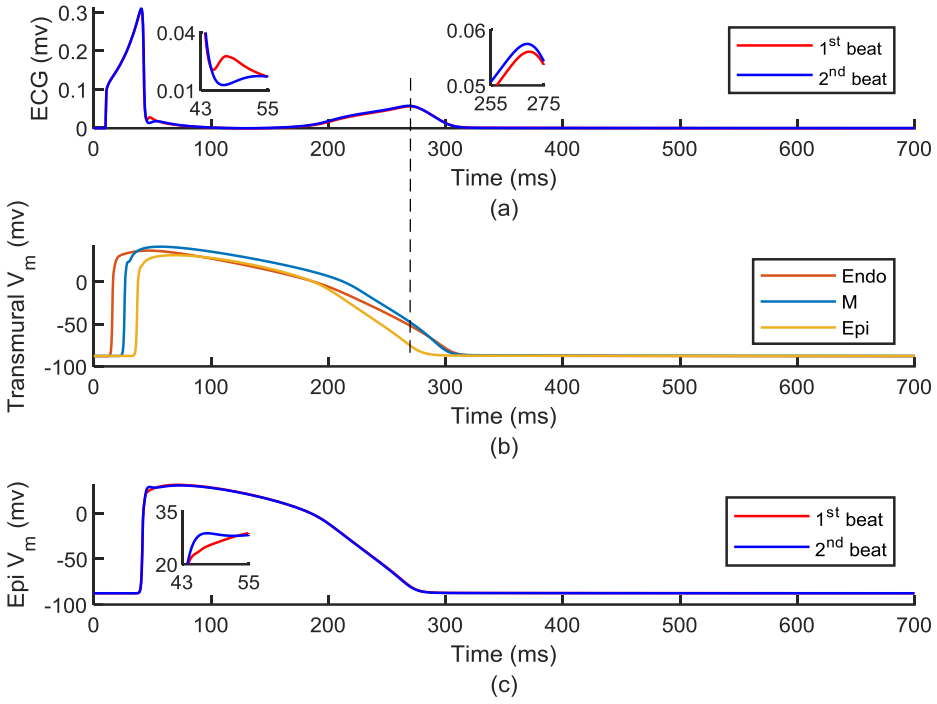

Figure 5. P-ECG and APDs during Epi ischemia. (a). Alternated p-ECG. (b). APDs of Endo cell (the 35th cell of the fiber), M cell (85th) and Epi cell (135th). (c). APDs of Epi (135th). Where O_r gate was added into Epi cell models.

Negative T wave arises from Endo ischemia (Figure 6a). Endo ischemia reduces repolarization durations of Endo cells due to I_{KATP} and leads Endo to complete repolarization earlier than M and Epi cells (Figure 6b). Under control, positive T wave is mainly determined by the positive vector starting from Endo to M cells. After APDs of Endo cells are reduced, the electrical vector becomes to point to Endo cell, which is opposite from the recording point of p-ECG, forming negative T wave.

TWA in type II is mainly centered on the first half of T waves (Figure 7a). Here, TWA could be divided into two phases, separated by the point A marked asterisk. Before point A, the second T wave is higher than the previous. After crossing the point, the second T wave becomes lower than the first. Meanwhile, APDs of Epi cells during the two beats almost intersect at the point A (Figure 7b). Comparing to the first beat, plateau phase in the second beat is longer and the whole repolarization duration is shorter. Longer plateau phase of Epi cells reduce the repolarization difference between Epi cell and Endo, M cells. In addition, the total reduced repolarization duration of Epi cell increases transmural repolarization heterogeneity.

Transmural ischemia reduces APDs of transmural cells and results in APD alternans in Endo, M and Epi cells (Figure 3). Evident TWA arises from cellular alternans among the whole cable (Figure 8). The changes of TWA magnitude and morphology are owing to altered repolarization heterogeneity. Different ischemic conditions (Table 1) shorten APD of transmural cells to different degrees. Here, T wave becomes negative, indicating APDs of Endo cells are shortened the most.

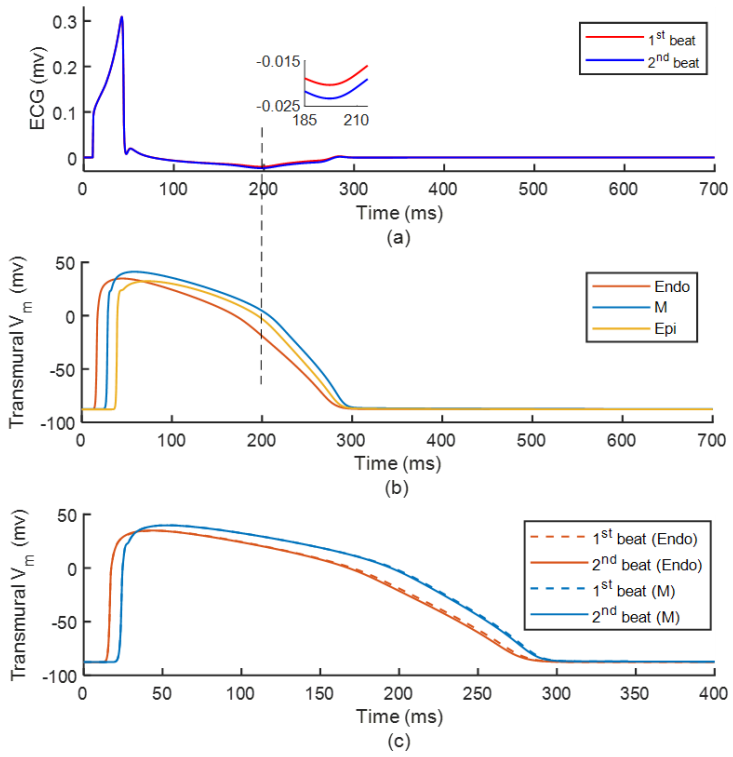

Figure 6. P-ECG and APDs during Endo ischemia. (a). Alternated p-ECG. (b). APDs of Endo cell (the 35th cell of the fiber), M cell (85th) and Epi cell (135th). (c). Alternated APD of Endo (35th) and M cells (65th). Where O_r gate was added into Endo cell model.

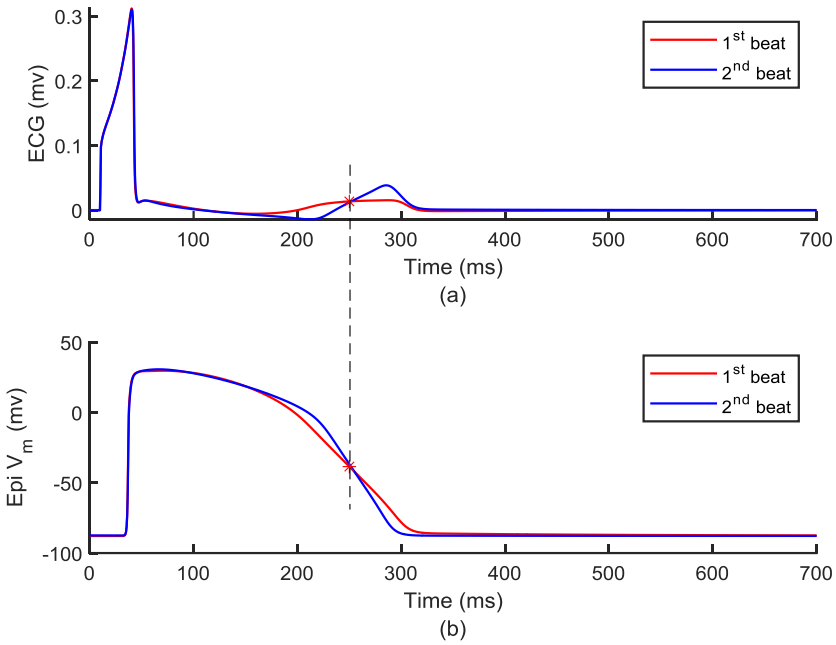

Figure 7. P-ECG and APDs in Epi ischemia. (a). Alternated p-ECG. (b). APDs of Epi cell (135th). Where τ_{rel} was increased in Epi cell model.

3.3. TWA with slow electrical conduction

Myocardial ischemia affects electrical conduction along myocardial fiber [44]. Here we simulated the effect of reduced conduction velocity on ECG in transmural ischemia. The duration of QRS increased obviously comparing to ECG in control conditions, resulting in ST and T wave postponed (Figure 9). The pattern and degree of TWA remained unchanged with slowing conduction velocity by comparing the two T waves in Figure 9.

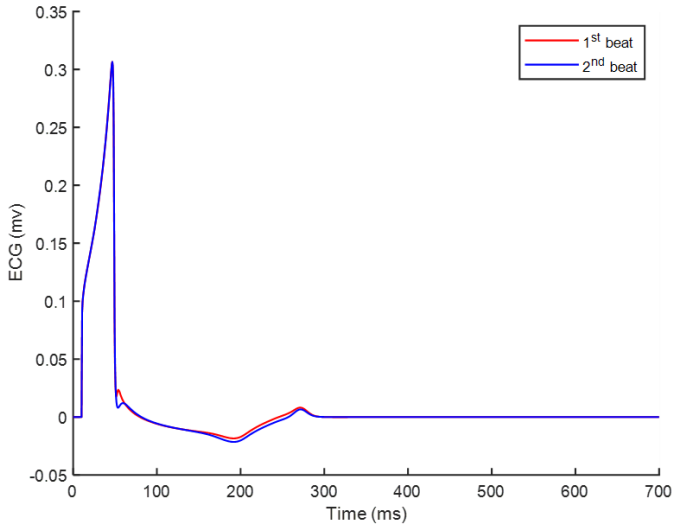

Figure 8. P-ECG in transmural ischemia, where O_r gates were added into transmural cell models.

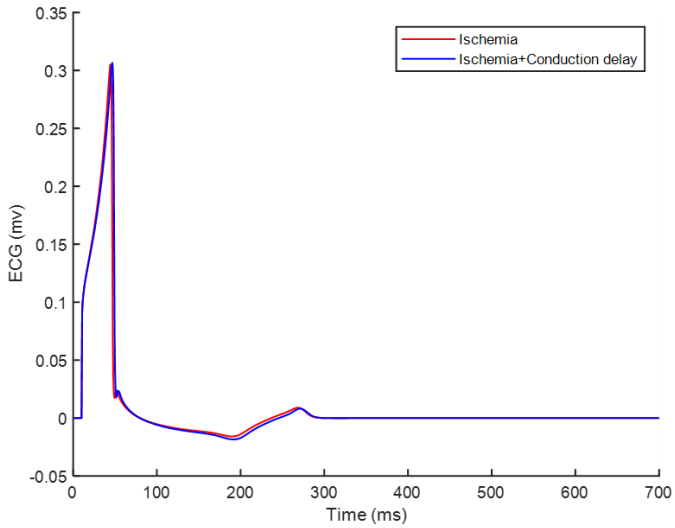

Figure 9. Under transmural ischemia, comparing p-ECG in control and slow conduction velocity. Where the velocity is reduced to 0.128 mm^2/ms.

4. Discussion

4.1. Ca^{2+} release in MI and Ca^{2+} alternans

Prolonging RyRs refractory would enhance Ca^{2+} alternans [45]. Vyacheslav et al [46] find that latency of Ca^{2+} release is prolonged after large Ca^{2+} transients and the restitution property of Ca^{2+} release makes a difference in forming alternans. In addition, secondary sparks are attributed to recruitment, a property of RyRs [43]. Investigators build a Ca^{2+} release model and prove that either increasing secondary sparks or prolonged Ca^{2+} release activities can lead to Ca^{2+} alternans [43]. In our simulations, we change the two properties separately and investigate their independent roles in contributing to cellular alternans. Although changes of either property could lead to Ca^{2+} alternans independently, the patterns of alternans in Ca^{2+} release current and Ca^{2+} transients are different.

Secondary sparks are the basis for forming Ca^{2+} waves. Propagation of Ca^{2+} waves is associated with Ca^{2+} alternans [43,47]. During Ca^{2+} alternans, the larger Ca^{2+} transient is confirmed to arise from Ca^{2+} waves propagation according to experimental measurements [47]. Previous studies prove the key role of $[Ca^{2+}]_{jsr}$ in forming Ca^{2+} alternans and Ca^{2+} waves [47,48]. When $[Ca^{2+}]_{jsr}$ is accumulated to a threshold, Ca^{2+} alternans will appear [48]. In alternans of type I, we simulate the effect of Ca^{2+} waves propagating, which is govern by O_r gate. When $[Ca^{2+}]_{jsr}$ reaches a "threshold", the gate becomes completely open (Figure 1e), producing large Ca^{2+} transients, which are like Ca^{2+} waves propagating. MI is shown to increase Ca^{2+} sparks frequency [49], however, the existence of the O_r gate has not been verified.

In type I, duration of Ca^{2+} release is short and the magnitude of Ca^{2+} release current alternates (Figure 1c). The alternating Ca^{2+} release activities are governed by the gate O_r. According to Eq 1, the value of O_r changes with $[Ca^{2+}]_{jsr}$. O_r in single cell model takes time to reach to its steady-state value and the time constant depends on I_{CaL}, which triggers Ca^{2+} release. Here, O_r was introduced to control magnitude of Ca^{2+} release current, mimicking alternating Ca^{2+} waves propagation.

In alternans of type II, τ_{rel} is increased. As RyRs are activated by I_{CaL}, the increased τ_{rel} leads to RyRs responding to I_{CaL} in every two beats. J_{rel} alternates obviously and release activities in the second beat can almost be ignored (Figure 1d). The very small Ca^{2+} release results in small amplitude of Ca^{2+} transients in the second beats (Figure 1b). Slow falling phase and broadening systolic peak of large Ca^{2+} transients are discernible, which coincides with previous studies [6,50,51]. Wu et al. [6] attribute the slow decay to decreased J_{up} in ischemia. Lee et al. [51] favor that broadening peak arises from Ca^{2+} release. In our simulations, the velocities of Ca^{2+} uptake in Ca^{2+} alternans of the two patterns are reduced by the same ischemic conditions. However, $[Ca^{2+}]_i$ decays slower in type II (Figure 1a,b). Our results indicated that broadening peak is mainly affected by prolonged Ca^{2+} released activities. In addition, experiments show that ischemia appears to result in contrasting changes of upstroke of $[Ca^{2+}]_i$ [6,51,52]. When the duration of ischemia is within 2.5 min, upstroke is found to be rapid [6,51]. After 4 h of ischemia, upstroke includes an initial rapid phase and a following slow phase [52]. Our upstroke (Figure 1b) slows down due to slow and sustained Ca^{2+} release.

4.2. The relationship between cellular alternans and TWA patterns

Ca^{2+} alternans of different patterns in ischemia result in different APD alternans and TWA patterns. In cellular alternans of type I, although Ca^{2+}-driven APD alternans are not evident, a long APD is

paralleled by a large Ca^{2+} transient, which is referred to as "in-phase" or "concordant" [21]. Conversely, type II Ca^{2+}-driven APD alternans are discordant. A large Ca^{2+} transient arises from a large Ca^{2+} release, leading to reduced I_{CaL}, increased I_{NaCa}, having contrast effects on APD. Where reducing I_{CaL} shortens plateau phase and increasing I_{NaCa} prolongs repolarization by extruding $[Ca^{2+}]_i$. Previous study [9,21,27] analyzes that whether Ca^{2+} alternans and APD alternans are concordant or discordant depends on which one of currents between I_{CaL} and I_{NaCa} plays a dominant role. In our simulation, the concordant alternans are due to the main effect of I_{NaCa} and the discordant alternans arise from the dominant role of I_{CaL}.

Note that in cable simulation, APD in the first beat is longer than in the second beat (Figure 7b). In single cell simulation, the first APD is shorter (Figure 2b). During Ca^{2+}-driven alternans forming TWA, coupling between neighboring cells also affects TWA morphology.

In control, there is slight difference in p-ECG morphology between two beats (Figure 4a). This is because the electrophysiological states of the cable are not so stable. The initial parameters of transmural cell models can make sure the cell model being in stable state during single cell simulation. Our cable simulation needs more time to come into stable with these parameters.

According to the insets in figure 5a and figure 6a, TWA can be induced by cellular alternans of type I. In cellular alternans of type II, TWA is obvious and its morphology is closely related with cellular alternans (Figure 7a,b). Although TWA induced by cellular alternans of type I is not evident, the magnitudes of TWA are larger than in control. In clinical, microvolt TWA is used to predict the risk of SCD [1,4,11]: When the value of TWA is higher than 46 μv [4], the risk of SCD and cardiac morality will rise sharply. In addition, experiments show that arrhythmia will occur when ischemia-induced TWA magnitude is 100-fold larger than in control [1]. TWA magnitude could not be recognized easily in clinical and simulations, it is meaningful to detect and evaluate the extent of alternans.

T wave magnitude increases during Epi ischemia (Figures 5a, 7a). APD of Epi is shorten by ischemia, resulting in larger repolarization dispersion within transmural cells (Figures 5b, 7b). T wave becomes negative during Endo ischemia and transmural ischemia (Figures 6a and 8a, b). Note that the maximum repolarization dispersion occurs earliest in transmural ischemia than in regional ischemia. The polarization of T wave along with the time points when T wave amplitudes arrive at can be used to identify ischemic zone.

In Epi ischemia, TWA concentrates in the first half of T waves (Figures 5a, 7a). The duration when TWA occur is confirmed to parallel the vulnerable period [41]. Similar findings are reported within a few minutes of occlusion [40]. Meanwhile, the second half of T waves remain uniform during consecutive beats [40]. However, within 2 to 10 days post-MI, alternans arises during the second half of T wave [53]. Our simulations of Endo ischemia and transmural ischemia show alternans exist during the total T wave (Figures 6a and 8a, b). According to these studies, the location of alternans in T wave on ECG can be linked to ischemic time or ischemic zone.

4.3. The effect of slowing conduction velocity on TWA

Conduction velocity is reduced by ischemia [44]. The slow electrical conduction interplays with cellular alternans to lead to spatial discordant alternans [16], which has ability to induce large TWA magnitude. Previous studies show the importance of T wave magnitude in ventricular arrythmia under MI [1,54]. Here we reduced conduction velocity and investigated the effect of slow conduction on TWA magnitude. In our simulations, slowing electrical conduction along the cable postponed ST and

T wave (Figure 9), however, T waves were postponed to the same extent during the two consecutive beats. Although our results favor that reduced conduction velocity has no effect on TWA pattern and magnitude, the conclusion still needs further investigation on 3D level.

Previous experiment shows activation delay increases from about 8 ms of control conditions to 35 ms in ischemic zone, which is identical during two consecutive beats [44]. Prolongation of activation time has been proven to have no effect on activation sequence and TWA magnitude [44]. Note that, delay of activation with slow conduction velocity leads to increased repolarization dispersion between ischemic zone and normal zone. The correlation between conduction and TWA magnitude should be fully investigated by simulating various reduced conduction velocity and ischemic zone.

A plethora of studies put forward that cardiac alternans in ischemia mainly arise from Ca^{2+} alternans [1,6,7,15,18]. Hyperkaleamia and slowed conduction play dominant roles in block, which also induce repolarization alternans [35]. As the effects of various ischemic factors on repolarization alternans are complex, cellular alternans and TWA under ischemia should be thoroughly studied.

Epi cells are proved to have a greater effect on TWA than M cells [22]. In our simulation, TWA in Epi ischemia (Figure 5a) is hardly to be detected, however, Endo ischemia leads to evident TWA (Figure 6a). Epi cells are closer to electrode than Endo cells, making bigger difference in forming TWA. However, various ischemic conditions should also be considered when analyzing the TWA magnitude. Ischemia leads to various Ca^{2+} alternans ratios, where the smallest Ca^{2+} alternans ratio is close to the boundary of ischemic zone [7]. Thus, more sever ischemia results in larger Ca^{2+} alternans ratio and correspondingly larger APD alternans. In addition, electrical coupling should also be considered in tissue simulation, which affects the cellular alternans pattern (Figure 7b). In our cable simulations, ischemic conditions were set more severe in Endo cells than Epi cells (Table 1). Correspondingly, in single cell simulations, ischemic Endo cell shows larger alternans in APD than ischemic Epi cell (Figure 3a,c).

5. Conclusions

Changes of RyR properties result in different Ca^{2+}-driven alternans and TWA patterns. Cellular alternans along with electrical coupling affect TWA morphology. Our simulations show the location of alternans in T wave can be associated with different ischemic zone. More analysis in terms of the location of TWA would provide useful insights to more detailed electrical changes during and after MI.

Reducing conduction velocity has no effect on TWA magnitude. However, slow conduction interplays with spatially concordant alternans to form SDA, indicating conduction velocity plays a key role in assisting other electrical factors to affect TWA.

6. Limitations

In our simulation, APD alternans induced by type I Ca^{2+} alternans are not obvious and thus TWA are not easy to be discernible. Changing ischemic settings or our formula of O_r gate may result in various APD alternans pattern. Other ischemic factors should be added to analyze TWA pattern thoroughly in the future.

Cellular concordant alternans induced by ischemia are simulated here, however, ECG of tissue with spatially discordant alternans could also provide deeply understanding in terms of the relationship

between APD alternans and TWA. We only could get more comprehensive conclusion after taking consideration of as many patterns of cellular alternans and TWA as possible.

Ischemic conditions in our simulation are set according to previous experimental data. However, our modification of J_{rel} is not based on experiments. We only consider if Ca^{2+} alternans ratios vary within reasonable range. In the future, more experimental data should be referenced and then furtherly modify the formula of J_{rel}.

More importantly, we only simulated p-ECG in one dimensional fiber. Investigation of TWA should be more valuable based on 3D-personalized cardiac model.

Acknowledgments

This work was supported by the Natural Science Foundation of China (NSFC) under grant number 61527811 and 61701435, the Key Research and Development Program of Zhejiang Province under grant number 2020C03016, the Zhejiang Provincial Natural Science Foundation of China under grant number LY17H180003, and the Medical Health Science and Technology Project of Zhejiang Provincial Health Commission under grant number 2020RC094.

Conflict of interest

The authors declare that there are no conflicts of interest.

References

1. R. L. Verrier, B. D. Nearing, Electrophysiologic Basis for T Wave Alternans as an Index of Vulnerability to Ventricular Fibrillation, *J. Cardiovasc. Electrophysiol.*, **5** (2010), 445–461.
2. V. Lakireddy, P. Baweja, A. Syed, G. Bub, M. Boutjdir, N. E. Sherif, Contrasting effects of ischemia on the kinetics of membrane voltage and intracellular calcium transient underlie electrical alternans, *Am. J. Physiol. Heart Circ. Physiol.*, **288** (2005), H400–H407.
3. B. Surawicz, C. Fisch, Cardiac alternans: diverse mechanisms and clinical manifestations, *J. Am. Coll. Cardiol.*, **20** (1992), 483–499.
4. M. U. Somuncu, H. Karakurt, Cardiac mortality predictability of T-wave alternans in young ST-elevated myocardial infarction patients with preserved cardiac function, *Turk Kardiyol Dern Ars*, **47** (2019), 449–457.
5. J. P. Martínez, S. Olmos, G. Wagner, P. Laguna, Characterization of repolarization alternans during ischemia: time-course and spatial analysis, *IEEE Trans. Biomed. Eng.*, **53** (2006), 701–711.
6. Y. Wu, W. T. Clusin, Calcium transient alternans in blood-perfused ischemic hearts: observations with fluorescent indicator fura red, *Am. J. Physiol. Heart Circ. Physiol.*, **273** (1997), H2161–H2169.
7. Y. Qian, W. T. Clusin, S. F. Lin, J. Han, R. J. Song, Spatial heterogeneity of calcium transient alternans during the early phase of myocardial ischemia in the blood-perfused rabbit heart, *Circulation*, **104** (2001), 2082–2087.
8. J. Hüser, Y. Wang, K. A. Sheehan, F. Cifuentes, S. L. Lipsius, L. A. Blatter, Functional coupling between glycolysis and excitation—contraction coupling underlies alternans in cat heart cells, *J. Physiol.*, **524** (2000), 795–806.

9. J. N. Edwards, L. A. Blatter, Cardiac alternans and intracellular calcium cycling, *Clin. Exp. Pharmacol. Physiol.*, **41** (2014), 524–532.
10. H. Hering, Das wesen des herzalternans, *Munch Med. Wochenschr*, **4** (1908),1417–1421.
11. R. L. Verrier, K. Kumar, B. D. Nearing, Basis for sudden cardiac death prediction by T-wave alternans from an integrative physiology perspective, *Heart Rhythm*, **6** (2009), 416–422.
12. T. Nieminen, R. L. Verrier, Usefulness of T-wave alternans in sudden death risk stratification and guiding medical therapy, *Ann. Noninvasive Electrocardiol.*, **15** (2010), 276–288.
13. S. M. Narayan, T-wave alternans and the susceptibility to ventricular arrhythmias, *J. Am. Coll. Cardiol.*, **47** (2006), 269–281.
14. M. L. Walker, D. S. Rosenbaum, Cellular alternans as mechanism of cardiac arrhythmogenesis, *Heart Rhythm*, **2** (2005), 1383–1386.
15. J. N. Weiss, A. Karma, Y. Shiferaw, P. S. Chen, A. Garfinkel, Z. Qu, From pulsus to pulseless: the saga of cardiac alternans, *Circ. Res.*, **98** (2006), 1244–1253.
16. M. A. Watanabe, F. H. Fenton, S. J. Evans, H. M. Hastings, A. Karma, Mechanisms for discordant alternans, *J. Cardiovasc. Electrophysiol.*, **12** (2001), 196–206.
17. E. Downar, M. J. Janse, D. Durrer, The effect of acute coronary artery occlusion on subepicardial transmembrane potentials in the intact porcine heart, *Circulation*, **56** (1977), 217–224.
18. W. T. Clusin, Mechanisms of calcium transient and action potential alternans in cardiac cells and tissues, *Am. J. Physiol. Heart Circ. Physiol.*, **294** (2008), H1–H10.
19. D. Sato, D. M. Bers, Y. Shiferaw, Formation of spatially discordant alternans due to fluctuations and diffusion of calcium, *PloS one*, **8** (2013), e85365.
20. E. Chudin, J. Goldhaber, A. Garfinkel, J. Weiss, B. Kogan, Intracellular Ca2+ dynamics and the stability of ventricular tachycardia, *Biophys. J.*, **77** (1999), 2930–2941.
21. Y. Shiferaw, D. Sato, A. Karma, Coupled dynamics of voltage and calcium in paced cardiac cells, *Phys. Rev. E*, **71** (2005), 021903.
22. D. Janusek, J. Svehlikova, J. Zelinka, W. Weigl, R. Zaczek, G. Opolski, et al., The roles of mid-myocardial and epicardial cells in T-wave alternans development: a simulation study, *Biomed. Eng. online*, **17** (2018), 1–21.
23. D. Sato, Y. Shiferaw, A. Garfinkel, J. N. Weiss, Z. Qu, A. Karma, Spatially discordant alternans in cardiac tissue: role of calcium cycling, *Circ. Res.*, **99** (2006), 520–527.
24. Y. Zang, L. Xia, Cellular mechanism of cardiac alternans: an unresolved chicken or egg problem, *J. Zhejiang Univ. Sci. B*, **15** (2014), 201–211.
25. G. Kanaporis, L. A. Blatter, The mechanisms of calcium cycling and action potential dynamics in cardiac alternans, *Circ. Res.*, **116** (2015), 846–856.
26. G. Kanaporis, L. A. Blatter, Membrane potential determines calcium alternans through modulation of SR Ca2+ load and L-type Ca2+ current, *J. Mol. Cell. Cardiol.*, **105** (2017), 49–58.
27. X. Wan, M. Cutler, Z. Song, A. Karma, T. Matsuda, A. Baba, et al., New experimental evidence for mechanism of arrhythmogenic membrane potential alternans based on balance of electrogenic INCX/ICa currents, *Heart Rhythm*, **9** (2012), 1698–1705.
28. S. Thakare, J. Mathew, S. Zlochiver, X. Zhao, E. G. Tolkacheva, Global vs local control of cardiac alternans in a 1D numerical model of human ventricular tissue, *Chaos,* **30** (8), 083123.
29. E. M. Cherry, Distinguishing mechanisms for alternans in cardiac cells using constant-diastolic-interval pacing, *Chaos*, **27** (2017), p.093902.

30. L. D. Szymanowicz, D. Kaufmann, K. Rozwadowska, M. Kempa, E. Lewicka, G. Raczak, Microvolt T-wave alternans and autonomic nervous system parameters can be helpful in the identification of low-arrhythmic risk patients with ischemic left ventricular systolic dysfunction, *PloS One*, **13** (2018), e0196812.
31. W. Ichiro, Effects of pinacidil on ST-T wave alternans during acute myocardial ischemia in the in-situ pig heart, *J. Nihon Univ. Med. Assoc.*, **76** (2017), 273–279.
32. Y. Zang, L. Dai, H. Zhan, J. Dou, L. Xia, H. Zhang, Theoretical investigation of the mechanism of heart failure using a canine ventricular cell model: Especially the role of up-regulated CaMKII and SR Ca2+ leak, *J. Mol. Cell. Cardiol.*, **56** (2013), 34–43.
33. J. M. Cordeiro, S. E. Howlett, G. R. Ferrier, Simulated ischaemia and reperfusion in isolated guinea pig ventricular myocytes, *Cardiovasc. Res.*, **28** (1994), 1794–1802.
34. P. Baumeister, T. A. Quinn, Altered calcium handling and ventricular arrhythmias in acute ischemia, *Clin. Med. Insights: Cardiology*, **10** (2016), CMC. S39706.
35. J. Liu, Y. Gao, Y. Gong, W. Xu, M. Jiang, L. Xia, One-dimensional simulation of alternating conduction under hyperkalaemic conditions, *Comput. Cardiol.,* **2017** (2017), 1–4.
36. J. M. Ferrero, J. Sáiz, J. M. Ferrero, N. V. Thakor, Simulation of action potentials from metabolically impaired cardiac myocytes: role of ATP-sensitive K+ current, *Circ. Res.*, **79** (1996), 208–221.
37. K. Tran, N. P. Smith, D. S. Loiselle, E. J. Crampin, Athermodynamic model of the cardiac sarcoplasmic/endoplasmic Ca2+ (SERCA) pump, *Biophys. J.*, **96** (2009), 2029–2042.
38. Y. Deng, J. Zhao, J. Yao, Q. Tang, L. Zhang, H. Zhou, et al., Verapamil suppresses cardiac alternans and ventricular arrhythmias in acute myocardial ischemia via ryanodine receptor inhibition, *Am. J. Transl. Res.*, **9** (2017), 2712–2722.
39. S. Kapur, J. A. Wasserstrom, J. E. Kelly, A. H. Kadish, G. L. Aistrup, Acidosis and ischemia increase cellular Ca2+ transient alternans and repolarization alternans susceptibility in the intact rat heart, *Am. J. Physiol. Heart Circ. Physiol.*, **296** (2009), H1491–H1512.
40. B. D. Nearing, S. N. Oesterle, R. L. Verrier, Quantification of ischaemia induced vulnerability by precordial T wave alternans analysis in dog and human, *Cardiovasc. Res.*, **28** (1994), 1440–1449.
41. B. D. Nearing, A. Huang, R. L. Verrier, Dynamic tracking of cardiac vulnerability by complex demodulation of the T wave, *Science*, **252** (1991), 437–440.
42. T. O'Hara, L. Virág, A .Varró, Y. Rudy, Simulation of the undiseased human cardiac ventricular action potential: model formulation and experimental validation, *PLoS Comput. Biol.*, **7** (2011), e1002061.
43. R. Rovetti, X. Cui, A. Garfinkel, J. N. Weiss, Z. Qu, Spark-induced sparks as a mechanism of intracellular calcium alternans in cardiac myocytes, *Circ. Res.*, **106** (2010), 1582–1591.
44. D. L. Carson, R. Cardinal, P. Savard, M. Vermeulen, Characterisation of unipolar waveform alternation in acutely ischaemic porcine myocardium, *Cardiovasc. Res.*, **20** (1986), 521–527.
45. X. Zhong, B. Sun, A. Vallmitjana, T. Mi, W. Guo, M. Ni, et al., Suppression of ryanodine receptor function prolongs Ca2+ release refractoriness and promotes cardiac alternans in intact hearts, *Biochem. J.*, **473** (2016), 3951–3964.
46. V. M. Shkryl, J. T. Maxwell, T. L. Domeier, L. A. Blatter, Refractoriness of sarcoplasmic reticulum Ca2+ release determines Ca2+ alternans in atrial myocytes, *Am. J. Physiol. Heart Circ. Physiol.*, **302** (2012), H2310–H2320.

47. M. E. Díaz, S. C. O'Neill, D. A. Eisner, Sarcoplasmic reticulum calcium content fluctuation is the key to cardiac alternans, *Circ. Res.*, **94** (2004), 650–656.
48. Y. Li, M. E. Díaz, D. A. Eisner, S. O'Neill, The effects of membrane potential, SR Ca2+ content and RyR responsiveness on systolic Ca2+ alternans in rat ventricular myocytes, *J. Physiol.*, **587** (2009), 1283–1292.
49. B. A. Cameron, K. Hiroaki, K. Kaihara, G. Iribe, T. A. Quinn, Ischemia enhances the acute stretch-induced increase in calcium spark rate in ventricular myocytes, *Front. Physiol.*, **11** (2020), 289–298.
50. J. Tomek, M. Tomková, X. Zhou, G. Bub, B. Roderiguez, Modulation of cardiac alternans by altered sarcoplasmic reticulum calcium release: a simulation study, *Front. Physiol.*, **9** (2018), 1306–1320.
51. H. C. Lee, R. Mohabir, N. Smith, M. R. Franz, W. T. Clusin, Effect of ischemia on calcium-dependent fluorescence transients in rabbit hearts containing indo 1. Correlation with monophasic action potentials and contraction, *Circulation*, **78** (1988), 1047–1059.
52. R. Tupling, H. Green, G. Senisterra, J. Lepock, N. McKee, Effects of ischemia on sarcoplasmic reticulum Ca2+ uptake and Ca2+ release in rat skeletal muscle, *Am. J. Physiol. Endocrinol. Metab.*, **281** (2001), E224–E232.
53. P. K. Stein, D. Sanghavi, P. P. Domitrovich, R. A. Mackey, P. Deedwania, Ambulatory ECG based T-wave alternans predicts sudden cardiac death in high risk post MI patients with left ventricular dysfunction in the EPHESUS study, *J. Cardiovasc. Electrophysiol.,* **19** (2008), 1037–1042.
54. T. Konta, K. Ikeda, M. Yamaki, K. Nakamura, K. Honma, I. Kubota, et al., Significance of discordant ST alternans in ventricular fibrillation, *Circulation*, **82** (1990), 2185–2189.

AIMS Press